

Nanoscale

Accepted Manuscript



This is an *Accepted Manuscript*, which has been through the Royal Society of Chemistry peer review process and has been accepted for publication.

Accepted Manuscripts are published online shortly after acceptance, before technical editing, formatting and proof reading. Using this free service, authors can make their results available to the community, in citable form, before we publish the edited article. We will replace this *Accepted Manuscript* with the edited and formatted *Advance Article* as soon as it is available.

You can find more information about *Accepted Manuscripts* in the [Information for Authors](#).

Please note that technical editing may introduce minor changes to the text and/or graphics, which may alter content. The journal's standard [Terms & Conditions](#) and the [Ethical guidelines](#) still apply. In no event shall the Royal Society of Chemistry be held responsible for any errors or omissions in this *Accepted Manuscript* or any consequences arising from the use of any information it contains.

Cite this: DOI: 10.1039/c0xx00000x

www.rsc.org/xxxxxx

ARTICLE TYPE

Precision improvement in dark-field microscopic imaging by using gold nanoparticles as internal reference: a combined theoretical and experimental study

Jun Ma,^a Yue Liu,^a Peng Fei Gao,^b Hong Yan Zou,^b and Cheng Zhi Huang^{*,a,b}²⁰ Received (in XXX, XXX) Xth XXXXXXXXX 20XX, Accepted Xth XXXXXXXXX 20XX

DOI: 10.1039/b000000x

Low accuracy is a big obstacle in dark-field microscopic imaging (iDFM) technique in practical applications. In order to reduce the deviations and fluctuations in the observed or snapped scattered light in iDFM technique caused by unavoidable measurement errors, bare gold nanoparticles (AuNPs) was introduced as an internal reference (IR). The feasibility of using AuNPs as IR in iDFM in theory was verified. The function of the IR in improving the precision of the acquired data through post data analysis was identified by three kinds of experiments: monitoring the oxidation process of silver nanoparticles (AgNPs) at room temperature, quantifying the level of glucose with AgNPs used as probes and quantifying the change in the light intensity of AuNPs after the plasmonic resonance energy transfer (PRET) between AuNPs and tetramethylrhodamine (TAMRA).

1 Introduction

Dark-field microscopic imaging (iDFM) technique is an effective tool to sensitively discern minute changes in the environment around plasmonic resonant nanoparticles (PRNs) which act as light scattering probes.¹⁻¹² In recent years, several research efforts have been focused on exploiting the optical properties of PRNs for achieving high sensitivity and resolution in iDFM technique.¹³⁻²⁰ Interesting physical, chemical and biological processes such as Brownian motion of single DNA molecules,¹³ the electrodeposition of silver nanoparticles (AgNPs),¹⁴ the click reaction,¹⁵ growth of nanoparticles,¹⁶ orientation dynamics of protein-coated gold nanorods,¹⁷ and transmembrane dynamics of nanoparticles¹⁸ can be monitored in real-time at the single-nanoparticle level by using iDFM technique. In addition to observing dynamic changes, iDFM technique can also be applied for quantifying targets when coupled with spectroscopic analysis. For example, cytochrome c has been detected based on selective plasmonic resonance energy transfer (PRET) between conjugated biomolecules and one single gold nanoplasmonic probe.¹⁹ Recently, ATP has been quantified with ultra-sensitivity and selectivity based on the principle that specific aptamer-ATP binding induced conformational change could modulate the surface-dependent self-catalytic growth of gold nanoparticles (AuNPs).²⁰

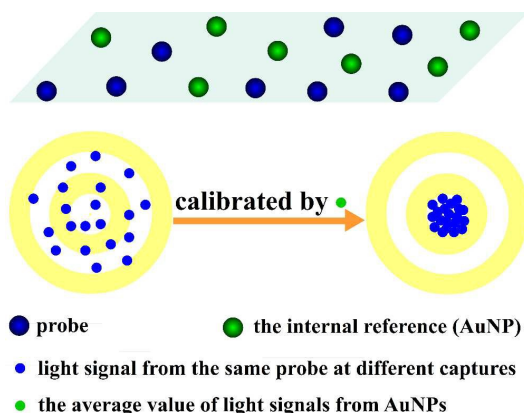
Despite its excellent features, iDFM technique still has some limitations including the low accuracy. There are several factors affecting the observed or snapped scattered light in iDFM technique in practical applications. Some of these factors, such as the light source, and the type of objective lens, can be controlled by manual operation, while the other factors, such as the distance between the dark-field condenser and the sample, the precise position of the dark-field condenser and the exact amount of oil

dropped on the condenser, cannot be fully controlled by manual operation. Although piezo electric devices with feedback loop can reduce some of these uncontrollable factors, such as the distance between the dark-field condenser and the sample, there are still uncontrollable factors which have a large influence on the acquired signals (the effect of oil dropped on the condenser is shown in Fig. S1 in the ESI†) and need to be adjusted by manual manipulation. When iDFM is used for detecting targets, achieving the light signals of probes before and after the addition of targets is necessary. Thus, the sample need to be captured followed by being removed from the microscope stage to contact targets and then replaced for the next capture. And during this process, large deviations caused by these uncontrollable factors as well as large fluctuations in the achieved signals will occur due to the incapacity for keeping the acquisition condition absolutely unchanged in these captures by manual manipulation. Large deviations caused by uncontrollable factors then make large unavoidable measurement errors which are hard to regulate until now.

In this study, we developed a new scheme in which an internal reference (IR) was introduced into iDFM technique to reduce the large fluctuations caused by the uncontrollable factors listed above. Although IR has been widely used in analytical techniques including mass spectrometry and chromatographic analysis, it has not been used as a solution for the low accuracy in iDFM technique until now. We chose AgNPs and the modified AuNPs as probes because of their high scattering efficiency and their wide applications,²¹⁻²³ while we chose the bare AuNPs herein as the IR because they have the advantageous properties of high scattering efficiency and convenient preparation.²⁴⁻²⁹ Furthermore, as an IR, the bare AuNPs should have to meet with

Nanoscale Accepted Manuscript

the four



Scheme 1 Illustration of the regulation process. The large deviations of the scattered light signals from probes caused by the unavoidable factors can be regulated by the average value of the scattered light signals from AuNPs which are used as the IR.

requirements: (1) be inert and not react with the target or interfere with the process for probing; (2) can be easily distinguished from the nanoparticles used as probes; (3) have similar diameters as probes so that they will be located in the same focal plane with probes when they are observed with DFM; (4) be able to work under the same conditions as probes.

Scheme 1 shows our working route wherein the large deviations in the achieved scattered light signals (herein they are the scattered light intensities) from the probes caused by the uncontrollable factors can be regulated by the average value of the scattered light signals from the bare AuNPs that was introduced as IR in iDFM technique. We found that the precision of the obtained experimental data from the probes could be greatly improved after the calibration of errors originating from adjustments of the relative position between sample and the dark-field condenser in the case of manual manipulation through post data analysis. Furthermore, small fluctuations in the acquired data were achieved thanks to the calibration of IR, making the quantification analysis by utilizing the change in the scattered light intensity of PRNs reliable in iDFM technique without the assistance of spectroscopic analysis, and greatly reducing the detection time from several minutes to several seconds.

2 Experimental section

2.1 Apparatus

A magnetic stirrer / hotplate with a temperature controller (HS40, Torrey Pines Scientific, USA) was used to precisely control the synthesis of AuNPs and AgNPs. The extinction spectrum for the prepared nanoparticles were measured by UV-Vis spectrophotometer (U-3010, Hitachi, Japan). A scanning electron microscope (SEM) (S-4800, Hitachi, Japan) was used to characterize the morphology of these nanoparticles. Dark-field microscopic images (iDFMs) were taken by an optical microscope (BX51, Olympus, Japan) equipped with a dark-field condenser (U-DCW, Olympus, Japan), a single chip true-color CCD camera (DP72, Olympus, Japan) and a 100 × objective lens. A 100 W halogen lamp was employed as the white light source to

excite the prepared nanoparticles, which then generated localized plasmon resonance scattering light.

2.2 Synthesis of AuNPs

AuNPs with average diameters of 54 nm and 13 nm were prepared according to previously reported procedures with slight modifications.^{30, 31} For preparing the 54 nm AuNPs, HAuCl₄ (0.5 wt %; 1 mL) and AgNO₃ (0.1 wt %; 42.5 μL) were added to 0.3 mL sodium citrate (1 wt %) under stirring. Water was added to bring the volume of the mixture solution up to 2.5 mL. The mixture was then incubated in a 25 °C water bath for 10 min. On the other hand, 47.5 mL water was stirred and heated to reflux, and then the mixture solution was quickly injected into the boiling water. The solution was further refluxed for 1 h under vigorous stirring, and then the heating was stopped. The 13 nm AuNPs were synthesized according to Frens' method. Briefly, HAuCl₄ (0.0385 wt %; 52 mL) was heated to reflux with vigorous stirring and then 1 mL sodium citrate (5 wt %) was quickly injected into the solution. The solution was kept under reflux for 15 min, and then cooled down. The prepared AuNPs were characterized by UV-Vis spectroscopy and SEM, and then used for iDFM measurements.

2.3 Synthesis of AgNPs

A modified route based on a literature procedure was used to prepare AgNPs with an average diameter of 27 nm.³² Briefly, a mixture of 20 mL water and 30 mL glycerol was vigorously stirred and heated up to 95 °C. Then, 9 mg AgNO₃ was added to the solvent. After one minute, 1 mL of sodium citrate (3 wt %) was quickly injected into the solution. The mixture was stirred at 95 °C for 1 h. After that, 20 μL AgNO₃ (0.1 g / mL) and 200 μL sodium citrate (3 wt %) were sequentially added to the mixture (time delay - 1 min), and this process was repeated 9 times (time delay - 5 min). After 0.5 h, the reaction was complete and the heating was stopped. The solution was further stirred for 1 h. The prepared AgNPs were characterized by UV-Vis spectroscopy, SEM, and used for iDFM.

2.4 Preparation of the tetramethylrhodamine (TAMRA) functionalized AuNPs

HS-ssDNA-TAMRA functionalized AuNPs were prepared according to the literature with slight modification.³³ DNA sequence: 5'-HS-GCACGAATTCACACG-TAMRA-3'. First, a small volume of tris(2-carboxyethyl) phosphine (TCEP) treated DNA solution (TCEP : DNA = 10 : 1, in 10 mM tris-HCl buffer, pH 7.4) was added into AuNPs solution (DNA : AuNPs = 2000 : 1) and mixed by a brief vortex. After ten minutes, 50 mM citrate.HCl buffer (pH 3, final 10 mM) was added into the AuNP solution. The solution was placed in dark for one hour.

2.5 Preparation of the mixture nanoparticles attached glass slides

Glass slides (25.4 × 76.2 mm, 1 - 1.5 mm in thick) were sequentially cleaned by chromic acid and distilled water, dried by nitrogen, and then immersed into 100 mL 0.05 % solution of 3-aminopropyltriethoxysilane (APTES) in acetone for 0.5 h. Then

the slides were washed three times with acetone, and finally dried at 70 °C for 2 h to obtain positively charged surfaces. After that, these APTES-modified glass slides were placed into a solution containing the mixture of negatively charged AgNPs and AuNPs for 30 minutes to absorb these nanoparticles by an electrostatic force.

2.6 The way for imaging the same nanoparticles by DFM and SEM

Firstly, a cross label was marked on one APTES-modified glass slide, and then the freshly prepared nanoparticles were fixed to the slide by an electrostatic attraction. One region nearby the marker was chosen and captured with DFM. In order to find the same region in the following visual field of SEM, the image captured by DFM should include one part of the cross label. Secondly, the visual field in SEM was amplified the same times as in DFM to quickly find the same region in SEM. The same region in SEM was found based on the same outline of the marker as in the DFM image and then SEM images were taken.

2.7 Evaluation the influence of IR on the precision improvement in monitoring dynamic processes

In order to assess the influence of IR on improving the precision of the acquired signals in monitoring dynamic processes, the oxidation process of AgNPs in air at room temperature was monitored. For achieving co-location of the same nanoparticles before and after their exposure to air, a cross label was marked on the APTES-modified glass slide and one region nearby the cross label was used. After the attachment of the freshly prepared AgNPs and AuNPs on this region by an electrostatic attraction, iDFMs of this region before and after the oxidation of these nanoparticles were taken. During the oxidation process, this region was directly exposed to air, and iDFMs of this region were taken (time delay - 15 min) until the light intensity of AgNPs was unchangeable. To be noticed, during the monitoring process, the slide was removed from the microscope after one capture of iDFM and then replaced just before the next iDFM was captured.

2.8 Evaluation the influence of IR on the precision improvement in quantifying targets

To evaluate the effect of IR on improving the precision of the acquired signals in quantifying targets, glucose was employed as the target for detection. AuNPs-13 nm can catalytically oxidize glucose in the presence of O₂, producing gluconic acid and H₂O₂ which can change the scattering light intensity of AgNPs. Thus, AuNPs-13 nm, AuNPs-54 nm, and AgNPs were used as the catalysis, IR and probes, respectively. For achieving co-location of the same nanoparticles before and after the reaction, a cross label was marked on each glass slide. After the attachment of the mixtures composed by AgNPs and AuNPs-54 nm by an electrostatic attraction, six marked glass slides were used and iDFMs of six regions nearby the cross labels corresponding to the six glass slides were captured, respectively. Then each slide was removed from the microscope stage and immersed into an open cell filled with 10 mL aqueous solution consisting of a mixture of glucose (with varied concentrations) and AuNPs-13 nm (0.335

nM, final concentration). It must be noted that the above solutions were prepared immediately prior to use. After one hour, each slide was removed from the cell, washed with distilled water and dried with nitrogen. iDFMs of the six chosen regions corresponding to the six slides were taken again.

3 Results and discussion

3.1 Identification of the feasibility for introducing AuNPs as the IR in iDFM technique in theory

Firstly, we measured light scattering features of the mixture nanoparticles composed by AgNPs and AuNPs. Due to the fact that the scattered light colors of AgNPs are dominated by blue (Fig. 1A and Fig. S2-1-Fig. S2-7 in the ESI†, up to 98 %) while those of AuNPs are dominated by green (Fig. 1B and Fig. S2-1-Fig. S2-7 in the ESI†, up to 80%), the nanoparticles scattering blue can be recognized as AgNPs while those scattering green as AuNPs in iDFMs of the mixtures containing AgNPs and AuNPs (Fig. 1C) and it would be used in the following investigations.

Then, we identified the feasibility of using the bare AuNPs as IR in iDFM technique while AgNPs were used to represent the probes. As stated above, both AuNPs and AgNPs should be imaged under the same conditions. After expressed as digital information from image through common software,³⁴ the average values of the scattered light intensities of all AgNPs (blue light, \bar{I}_{blue}) and AuNPs (green light, \bar{I}_{green}) from these images could be available. In order to make AuNPs function as a suitable IR, the ratio of $\bar{I}_{\text{blue}} / \bar{I}_{\text{green}}$ obtained from the same region at different captures should be constant unless chemical reactions or physical changes occur and factors which have the possibility to affect the ratio of $\bar{I}_{\text{blue}} / \bar{I}_{\text{green}}$ should be tested. Thus, iDFM of the mixture of AuNPs and AgNPs in the same region was continuously captured 8 times, during which the uncontrollable factors were tested by

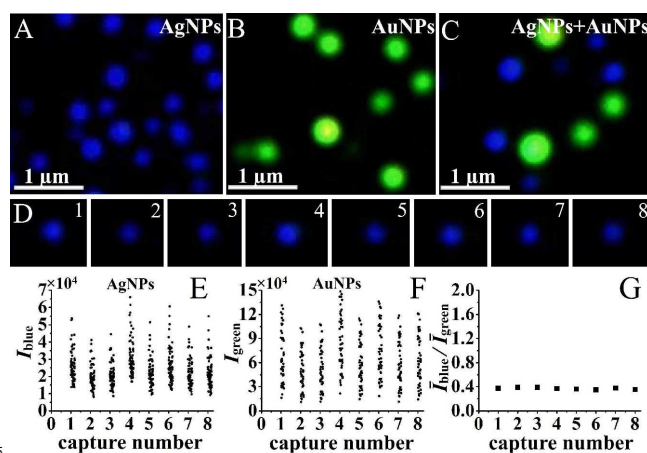


Fig. 1 Identification of the feasibility of introducing the bare AuNPs as the IR in iDFM technique. (A), (B) and (C), iDFMs of AgNPs, AuNPs and the mixture of AgNPs and AuNPs, respectively. (D) The scattered light of the same single AgNP from 8 captures. (E) and (F) are the light intensities of same 50 AgNPs and AuNPs in 8 captures, respectively. The mixture of AgNPs and AuNPs were absorbed on a region by an electrostatic attraction. The 50 AgNPs and AuNPs were randomly selected from the mixture nanoparticles to represent all AgNPs and AuNPs in this region, respectively. (G) The ratio of $\bar{I}_{\text{blue}} / \bar{I}_{\text{green}}$ for the 8 captures, wherein \bar{I}_{blue} and \bar{I}_{green} are the average values of the 50 randomly

selected AgNPs (E) and AuNPs (F), respectively.

deliberately shifting the AuNPs and AgNPs loaded slide. That is, the slide was removed from the microscope stage after one capture of iDFM and replaced just before the next capture to make the relative position between sample and the dark-field condenser keep changing. During this factitious process, the slide was not subjected to further chemical reactions or physical changes.

Accordingly, 8 iDFMs were achieved after 8 captures. Fig. 1D shows the typical fluctuations in light signals of the same single AgNP from 8 iDFMs. The same 50 spherical but not too bright blue spots and green spots were randomly selected in these iDFMs to represent the scattering features of all single nanoparticles scattering blue (AgNPs) and green (AuNPs), respectively. All these chosen light spots could be digitalized and 8 columns reflecting the large fluctuations in the achieved signals caused by uncontrollable factors were obtained (Fig. 1E, 1F). In order to achieve reliable results and make the sample unbiased representative of the whole, all typical nanoparticles used in this study should be randomly selected and evenly distributed in the whole image (see 3 in the ESI†).

The average values of the light intensities of the 50 selected nanoparticles (\bar{I}_{blue} and \bar{I}_{green}) were calculated. As shown in Fig. 1G, the ratio of $\bar{I}_{\text{blue}} / \bar{I}_{\text{green}}$ is about 0.4, and it remains unchanged in the absence of further chemical reactions or physical changes, indicating that the introduction of the bare AuNPs as IR in iDFM technique is feasible and reliable.

3.2 Introduction of the calibration factor α

Having confirmed the feasibility of the bare AuNPs as IR in iDFM technique, we further introduced a calibration factor based on the inert features of IR, α , to reduce the unavoidable errors in the acquired signals of AgNPs (as the representative of the probes) resulting from uncontrollable factors during the manual operation (for further information, see 4 in the ESI†)

$$\alpha = \frac{\bar{I}_{\text{green}}}{\bar{I}_{\text{green}}'} \quad (1)$$

Wherein \bar{I}_{green} and \bar{I}_{green}' represent the average values of the obtained intensities of the green scattered light from the bare AuNPs before and after chemical reactions or physical changes.

3.3 Evaluation the function of IR in improving the precision of the acquired data in monitoring dynamic processes

In order to identify the applicability of the bare AuNPs acting as an IR to calibrate errors caused by uncontrollable factors in monitoring dynamic processes, we monitored the oxidation process of AgNPs in air at room temperature. As is well known, AgNPs are sensitive to the surroundings, and the easy but slow oxidation of Ag (0) to Ag₂O in air can result in the decrease in the light scattering intensity of AgNPs due to the fact that the plasmon resonance of AgNPs can be significantly affected by the presence of Ag oxides on their surfaces.³⁵ Thus, we could monitor the change in the average value of the scattered light intensities of AgNPs in the same region. iDFMs of the same region before and after the oxidation of AgNPs in air were captured at an interval of 15 min, and 9 iDFMs were obtained

(see 5 in the ESI†). To be mentioned, this process was executed

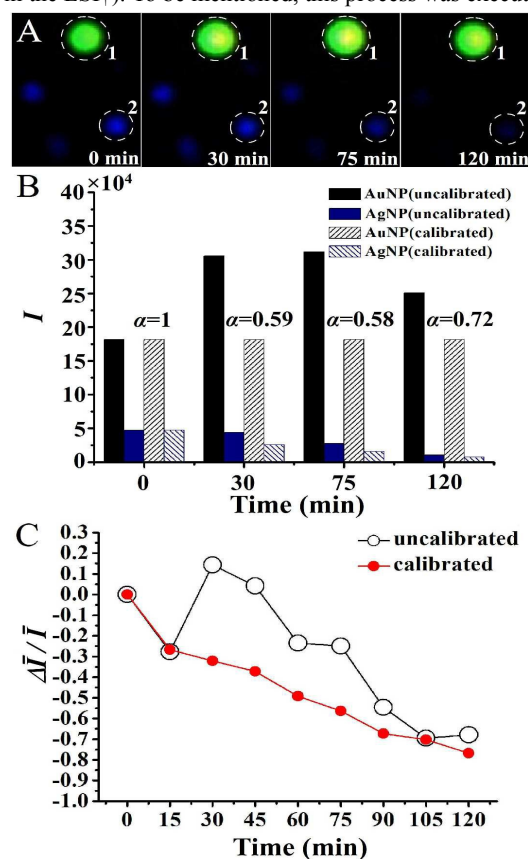


Fig. 2 Monitoring the oxidation of AgNPs in air at room temperature. iDFMs of the same region before and after the oxidation of AgNPs were captured and used. (A) iDFMs of the mixture composed of AuNP (the green spot) and AgNPs (the blue spots) after their exposure to air for 0 different time. These iDFMs are parts of the iDFMs of the whole region. (B) The average values of the light intensities of AuNPs (from the whole region) and the light intensities of AgNP (from Fig. 2A, marked by number 2) at different exposure time in air before and after calibration. (C) The change in $\Delta I / I$ with increasing the exposure time of AgNPs in air before (black curve with hollow circles) and after (red curve with solid circles) calibration. \bar{I} is the average value of the light intensities of AgNPs from the whole region at the beginning and ΔI represents the change of the average value of the intensities of AgNPs from the whole region after their exposure in air.

in the presence of the unavoidable errors resulted from adjustments of the relative position between sample and the dark-field condenser.

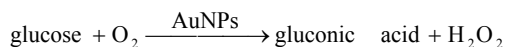
As shown in Fig. 2A, the intensity of the green light from one single AuNP (marked by number 1) was changing and the latter three green spots were brighter than the first one, indicating that large fluctuations in the acquired signals originating from unavoidable errors had occurred since AuNPs attached on glass slide are stable in air (see next and Fig. 3, even when they were mixed with H₂O₂, they are stable). Although the scattered light intensity of the blue light from one single AgNP (marked by number 2) was decreasing with the increasing exposure time in air, the data was still unreliable considering the large fluctuations. In such case, α was employed for calibrating these large deviations through post data analysis. According to Eq. (1), α could be calculated with the average value of the light intensities of AuNPs at the beginning (\bar{I}_{green}) and the other exposure time

(\bar{I}_{green}). Then the light intensities of AgNP from Fig. 2A (Fig. 2B, the blue solid columns) at four different exposure time in air were calibrated by multiplying the value of α (Fig. 2B, the blue diagonal stripe columns).

Furthermore, the average values of the light intensities of AgNPs from the whole image region could also be calibrated. \bar{I} is the average value of the light intensities of AgNPs at the beginning, while $\Delta\bar{I}$ is the change in the average value of the intensities of AgNPs. As seen in Fig. 2C, before calibration, $\Delta\bar{I}/\bar{I}$ was found to be irregular with the increasing exposure time in air (black curve with hollow circles). After α was employed, the calibrated $\Delta\bar{I}/\bar{I}$ was decreased with the increasing exposure time in air (red curve with solid circles), showing much more regular and reasonable results. Therefore, we could conclude that surface oxidation of AgNPs could be precisely monitored by using the bare AuNPs as IR in iDFM technique even without the use of in-situ probing.

3.4 Evaluation the function of IR in improving the precision of the acquired data in quantifying targets

To evaluate the influence of IR on improving the precision of the acquired data in quantifying targets, we applied the bare AuNPs as IR in iDFM technique to quantify chemical reactions. Glucose was selected as a typical target considering its high importance in life activities.³⁶ Glucose was detected by combining the glucose oxidase (GOx)-mimicking activity of AuNPs-13 nm and the sensitivity of AgNPs to H_2O_2 .



Then the resulted H_2O_2 can easily oxidize AgNPs and lead to the decrease in the light intensity of AgNPs. Based on this, glucose can be quantified with iDFM technique.

In order to reveal the mechanism for the reaction between AgNPs and H_2O_2 , DFM and SEM were combined to co-locate the same nanoparticles before and after the reaction.⁴ As Fig. 3A-3E (see 6 in the ESI†) show, as an IR, the AuNPs had neither the change in the scattered light intensity nor the change in the morphology even after long-term exposure to H_2O_2 . After exposed to H_2O_2 , the blue scattered light from AgNPs as measured by DFM diminished (Fig. 3C, 3D), while their morphologies scarcely changed as observed by SEM (Fig. 3B, 3E, and 7 in the ESI†). We supposed that the reduction in the intensity of the blue light was due to the fact that the Ag_2O shell formed on the surface of AgNPs affected the plasmon resonance of these AgNPs,³⁵ causing great decrease of the scattered light.

Fig. 4 shows the relationship between the relative change in the average value of the light intensities of AgNPs ($\Delta\bar{I}/\bar{I}$) and the concentration of glucose (c) for the detection of glucose. Without calibration (the black curve), the first three points were irrational because it was unreasonable that the second and third points were larger than the first point, indicating the light intensity of AgNPs were increased after exposing AgNPs to glucose. As a consequence, the overall trend of the curve deviated from the actual and the result was unreliable.

Having confirmed that the scattered light of AuNPs would not change during the detection process (see 8 in ESI†), AuNPs were used to make sure that the change in the light intensity of AgNPs

was precise. After calibrated by α in post data analysis (Fig. 4, the

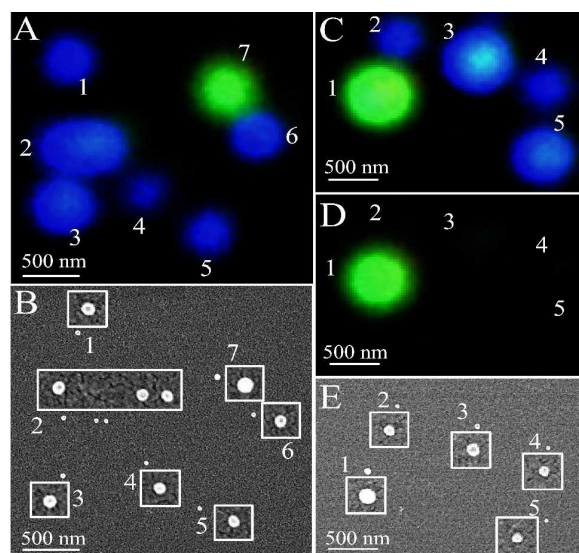


Fig. 3 Characterization of the mixture of AgNPs and AuNPs before (A-C) and after (D, E) their interaction with H_2O_2 . (A, C, D) iDFMs of these nanoparticles. (B, E) SEM images of the same nanoparticles as in Fig. 3A and 3D, respectively. (C, D) iDFMs of the mixture nanoparticles from the same region before (C) and after (D) their exposure to H_2O_2 .

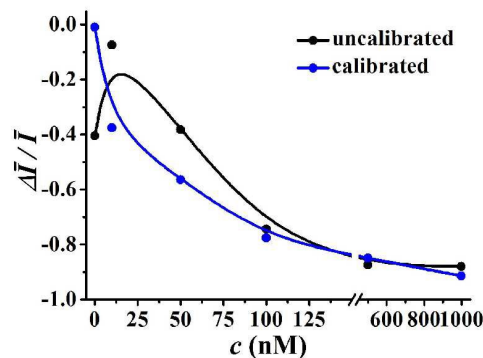


Fig. 4 Detection of glucose with AgNPs as calibrated by AuNPs. $\Delta\bar{I}/\bar{I}$ as a function of the concentration of glucose (c) before (the black curve) and after (the blue curve) being calibrated with α . \bar{I} is the average value of the light intensities of AgNPs from the whole image region at the beginning and $\Delta\bar{I}$ represents the change in the average value of the intensities of AgNPs from the whole region after the reaction.

blue curve), the curve became much more regular and reasonable since the formed Ag_2O shell on AgNPs can lead to the decrease in the scattered light of AgNPs. When the concentration of glucose (c) varied from 10 nM to 100 nM, the $\Delta\bar{I}/\bar{I}$ showed a sharp decrease, and after that, the change of $\Delta\bar{I}/\bar{I}$ was much more even.

3.5 The flexibility of the IR in practical applications

In practical applications, the probes used in iDFM technique are not just limited to AgNPs and they can also be AuNPs. In such case, the bare AuNPs can be chosen as the IR while the functionalized AuNPs are chosen as the probes. For example, in order to investigate the plasmonic resonance energy transfer (PRET) between AuNPs and TAMRA, AuNPs modified with HS-ssDNA-TAMRA (AuNPs-TAMRA) were used as the probes.

Since both the bare AuNPs and the AuNPs-TAMRA have the

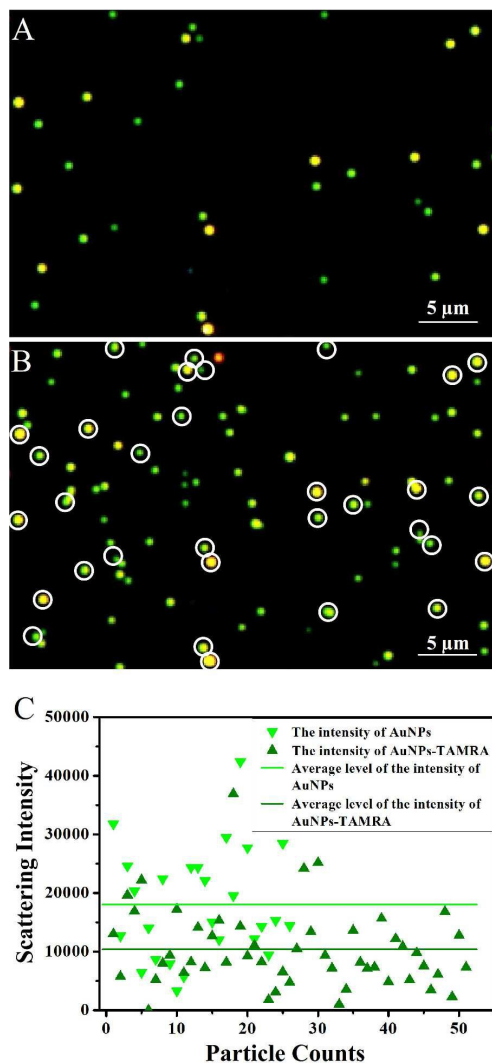


Fig. 5 The bare AuNPs as the IR when AuNPs-TAMRA were the probes. (A) iDFM of AuNPs. (B) iDFM of AuNPs (marked by the white circles) and AuNPs-TAMRA. (C) The scattered light intensities of AuNPs and AuNPs-TAMRA from 5B.

green scattering light, in order to distinguish them, the bare AuNPs were firstly fixed on the glass slide, one region on the slide was captured (as seen in Fig. 5A). Then AuNPs-TAMRA were fixed to the same glass slide, and the same region was captured again (as seen in Fig. 5B). In Fig. 5B, the light spots marked by white circles can be identified as the bare AuNPs while the rest of the spots as the AuNPs-TAMRA. After expressed as digital information from Fig. 5B, the scattered light intensities of AuNPs and AuNPs-TAMRA are shown in Fig. 5C. The average level of the scattered light intensities of them were 18030 and 10384, respectively. In other words, the strong absorbance of TAMRA in 550 nm reduced the scattering light of AuNPs which had a peak at ~550 nm by more than 42 %.

Besides, the IR used in iDFM technique is not just limited to gold nanospheres, and gold nanoparticles with other geometry, such as nanorods and nanocubes can also be used as the IR.

Except for AuNPs, many non-plasmonic materials, such as submicron polymer beads, can be used as the IR as long as they meet the four requirements which have been described in the last sentence of the third paragraph. The IR is flexible and it can be changed as the change of probes.

4 Conclusions

In summary, the bare AuNPs was introduced to iDFM technique as an IR for the first time to reduce the large unavoidable errors caused by uncontrollable factors in post data analysis, and improved precision of the acquired signals from AgNPs or functionalized AuNPs acting as probes has been obtained. The feasibility of this method was validated and then a calibration factor (α) was introduced to reduce fluctuations in signals of the probes. The improved precision by using AuNPs as IR has been identified by monitoring the oxidation process of AgNPs in air at room temperature, quantifying the level of glucose, and quantifying the change in the light intensity of AuNPs after the PRET between AuNPs and TAMRA in the presence of the unavoidable errors. To be mentioned, the IR is flexible, and many materials¹⁸ can act as the IR providing they meet the four requirements which have been listed above. Furthermore, the small fluctuations in the acquired data make the quantification analysis by utilizing the change of the scattered light intensity of PRNs reliable in iDFM technique without the assistance of spectroscopic analysis, greatly reducing the detection time from several minutes to several seconds. We believe that the IR can find wide applications in monitoring some processes which cannot be accomplished in-situ and quickly quantifying fast reactions in iDFM technique.

Acknowledgements

All authors greatly appreciate the financial supports from the National Natural Science Foundation of China (NSFC, 21535006).

Notes and references

- ^a Key Laboratory of Luminescent and Real-Time Analytical Chemistry, Ministry of Education, College of Chemistry and Chemical Engineering, Southwest University, Chongqing 400715, China. E-mail: chengzhi@swu.edu.cn; Fax: +86 23 68367257; Tel: +86 23 68254659
^b Chongqing Key Laboratory of Biomedical Analysis (Southwest University), Chongqing Science & Technology Commission, College of Pharmaceutical Science, Southwest University, Chongqing 400716, China.

† Electronic Supplementary Information (ESI) available: [details of any supplementary information available should be included here]. See DOI: 10.1039/b000000x/

- X. Xu, Y. Chen, H. Wei, B. Xia, F. Liu and N. Li, *Anal. Chem.*, 2012, **84**, 9721-9728.
- B. Xiong, R. Zhou, J. Hao, Y. Jia, Y. He and E. S. Yeung, *Nat. Commun.*, 2013, **4**, 1708.

3. X. Xu, T. Li, Z. Xu, H. Wei, R. Lin, B. Xia, F. Liu and N. Li, *Anal. Chem.*, 2015, **87**, 2576-2581. 21.
4. Y. Liu and C. Z. Huang, *Nanoscale*, 2013, **5**, 7458-7466. 40 22.
5. L. Zhang, Y. Li, D.-W. Li, C. Jing, X. Chen, M. Lv, Q. Huang, 23.
- 5 Y.-T. Long and I. Willner, *Angew. Chem. Int. Ed.*, 2011, **50**, 6789-6792.
6. J. J. Mock, M. Barbic, D. R. Smith, D. A. Schultz and S. 24.
- Schultz, *J. Chem. Phys.*, 2002, **116**, 6755-6759. 45
7. C. Sonnichsen, T. Franzl, T. Wilk, G. von Plessen, J. 25.
- 10 Feldmann, O. Wilson and P. Mulvaney, *Phys. Rev. Lett.*, 2002, **88**, 077402-077402.
8. L. S. Slaughter, Y. Wu, B. A. Willingham, P. Nordlander and S. 26.
- Link, *ACS Nano*, 2010, **4**, 4657-4666. 50
9. W. Ni, T. Ambjörnsson, S. P. Apell, H. Chen and J. Wang, 27.
- 15 *Nano Lett.*, 2009, **10**, 77-84.
10. L. Slaughter, W.-S. Chang and S. Link, *J. Phys. Chem. Lett.*, 28.
- 2011, **2**, 2015-2023.
11. M. A. Mahmoud and M. A. El-Sayed, *J. Phys. Chem. Lett.*, 55 29.
- 2013, **4**, 1541-1545.
- 20 12. L. Lermusiaux, V. Maillard and S. Bidault, *ACS Nano*, 2015, 30.
- 9**, 978-990.
13. K. Hirano, T. Ishido, Y. S. Yamamoto, N. Murase, M. 31.
- Ichikawa, K. Yoshikawa, Y. Baba and T. Itoh, *Nano Lett.*, 60 32.
- 2013, **13**, 1877-1882.
- 25 14. C. M. Hill and S. Pan, *J. Am. Chem. Soc.*, 2013, **135**, 17250- 33.
- 17253.
15. L. Shi, C. Jing, W. Ma, D.-W. Li, J. E. Halls, F. Marken and 34.
- Y.-T. Long, *Angew. Chem. Int. Ed.*, 2013, **52**, 6011-6014. 65
16. Y. Liu and C. Z. Huang, *ACS Nano*, 2013, **7**, 11026-11034. 35.
- 30 17. D. Xu, Y. He and E. S. Yeung, *Angew. Chem. Int. Ed.*, 2014, 37.
- 53**, 6951-6955.
18. D. Xu, Y. He and E. S. Yeung, *Anal. Chem.*, 2014, **86**, 3397- 36.
3404. 70
19. G. L. Liu, Y.-T. Long, Y. Choi, T. Kang and L. P. Lee, *Nat. 37.*
- 35 *Meth.*, 2007, **4**, 1015-1017.
20. Q. Liu, C. Jing, X. Zheng, Z. Gu, D. Li, D.-W. Li, Q. Huang, 37.
- Y.-T. Long and C. Fan, *Chem. Commun.*, 2012, **48**, 9574-9576. 37.
- P. F. Gao, B. F. Yuan, M. X. Gao, R. S. Li, J. Ma, H. Y. Zou, Y. F. Li, M. Li and C. Z. Huang, *Sci. Rep.*, 2015, **5**, 15427.
- Y. Xianyu, J. Sun, Y. Li, Y. Tian, Z. Wang and X. Jiang, *Nanoscale*, 2013, **5**, 6303-6306.
- Y. Tian, J. Qi, W. Zhang, Q. Cai and X. Jiang, *ACS Appl. Mater. Inter.*, 2014, **6**, 12038-12045.
- C. D. Medley, J. E. Smith, Z. Tang, Y. Wu, S. Bamrungsap and W. Tan, *Anal. Chem.*, 2008, **80**, 1067-1072.
- X. Zheng, Q. Liu, C. Jing, Y. Li, D. Li, W. Luo, Y. Wen, Y. He, Q. Huang, Y.-T. Long and C. Fan, *Angew. Chem. Int. Ed.*, 2011, **50**, 11994-11998.
- L. A. Austin, B. Kang and M. A. El-Sayed, *J. Am. Chem. Soc.*, 2013, **135**, 4688-4691.
- C. Jing, Z. Gu, Y.-L. Ying, D.-W. Li, L. Zhang and Y.-T. Long, *Anal. Chem.*, 2012, **84**, 4284-4291.
- Y. Zhao, Y. Tian, Y. Cui, W. Liu, W. Ma and X. Jiang, *J. Am. Chem. Soc.*, 2010, **132**, 12349-12356.
- Y.-F. Huang, H.-T. Chang and W. Tan, *Anal. Chem.*, 2008, **80**, 567-572.
- H. Xia, S. Bai, J. r. Hartmann and D. Wang, *Langmuir*, 2009, **26**, 3585-3589.
- G. Frens, *Nat. Phys. Sci.* 1973, **241**, 20-22.
- D. Steinigeweg and S. Schlucker, *Chem. Commun.*, 2012, **48**, 8682-8684.
- X. Zhang, M. R. Servos and J. Liu, *J. Am. Chem. Soc.*, 2012, **134**, 7266-7269.
- Y. Liu and C. Z. Huang, *Chem. Commun.*, 2013, **49**, 8262-8264.
- N. Grillet, D. Manchon, E. Cottancin, F. Bertorelle, C. Bonnet, M. Broyer, J. Lermé and M. Pellarin, *J. Phys. Chem. C*, 2013, **117**, 2274-2282.
- J. Castillo, S. Gáspár, S. Leth, M. Niculescu, A. Mortari, I. Bontidean, V. Soukharev, S. A. Dorneanu, A. D. Ryabov and E. Csöregi, *Sens. Actuators B*, 2004, **102**, 179-194.
- L.-X. Qin, C. Jing, Y. Li, D.-W. Li and Y.-T. Long, *Chem. Commun.*, 2012, **48**, 1511-1513.